

EUVE Investigation of Three Short-Period Binary Stars

SLAVEK M. RUCINSKI

Eureka Scientific Inc.

2452 Delmer St., Oakland, CA 94602-3017

August 9, 2018

ABSTRACT

EUVE satellite spectroscopic observations (SW, MW and LW bands covering 80 – 160, 170 – 350 and 450 Å with resolutions 0.5, 1 and 2 Å) and photometric observations (Deep Sky Survey, broad-band 70 – 140 Å) have been obtained for two contact, 44i Boo B and VW Cep, and one detached, ER Vul, close binary stars. All three systems have orbital periods shorter than one day and thus are expected to show “saturated” levels of chromospheric, transition-region and lower-corona emissions. The spectroscopic data were of sufficient quality for an attempt at an emission-measure determination only for 44i Boo B. This determination, based entirely on iron lines, and utilizing Singular Value Decomposition formalism developed by Schmitt et al. (1996) indicates lack of any dominating temperature regime with the emission measure rising from $\log T \simeq 6$ to $\log T \simeq 7.2$. However, strong dependence of the resulting emission-measure curve on the inclusion of individual lines formed at high temperatures casts some doubts about the quality of the solution. A comparison of the line strengths have been made for selected strongest chromospheric, transition-region and lower-coronal emission lines; it included the data for the single, rapidly-rotating star AB Dor which is the only such star with the rotation period shorter than one day which has been observed with the EUVE. If the single-epoch observations are representative, the results indicate that AB Dor is under-active relative to the three binary stars which show similar levels of activity.

Subject headings: binaries: close — binaries: eclipsing

1. INTRODUCTION: VERY CLOSE BINARY STARS

Very close, synchronized, late spectral-type binaries offer us laboratories of stars that are forced to rotate much more rapidly than would be normally encountered among late-type stars. Except for very young stars which still contain large amounts of original angular momentum from recent formation, old stars of the F, G and K spectral types tend – on the average – to rotate progressively less rapidly with the advancing spectral type due to increased efficiency of the magnetic-wind braking for lower effective temperatures. Contact binary systems are a most

interesting exception in this respect as they obey the orbital period – color relation which is just opposite to this trend, with the cooler stars rotating more rapidly. This unusual combination leads to a very large range in observed levels of magnetic activity among contact binaries, with highest levels well in the saturated regime (Vilhu & Walter 1987). Two such systems are the subject of this paper. They are compared with a very close, but detached binary and with a single, rapidly-rotating young star. All four stars have rotation periods shorter than one day.

There have been several reviews about contact binaries (Rucinski 1985a, 1993) and about some aspects of their magnetic activity (Rucinski 1985b). At this point it is sufficient to stress that, although these are binary stars, they should be considered as single entities from the point of view of their internal structure because of the on-going (but hidden to observers) processes of mass and energy exchange between the components. These internal processes of energy and mass transfer within such structures are poorly understood, but this seems to be of relatively minor importance for characterization of activity of contact binaries which tends to follow the basic trends established for non-contact stars. It is of relevance that periods and colors of contact systems correlate as expected for components that are not too distant from the Main Sequence: the small, short-period systems have low temperatures whereas the long-period systems are relatively hot and bright. The sharp, currently unexplained, short-period cutoff in the period distribution is observed at 0.22 day corresponding to spectral type K5. Most of the contact systems have orbital periods concentrated within $0.25 < P < 0.5$ day where the spectral types range between middle K and late A, with few reaching periods of one day where the spectral types are middle A. Such contact systems are called the W UMa-type binaries, in contrast to the continuation of this sequence to early-type contact binaries, with periods of a few days and spectral types as early as O-type. The latter are of no interest in the present context, so that in this paper the names of W UMa-type and contact binaries will be used interchangeably.

The new results based on the statistics for a volume-limited sample of the contact systems in the OGLE micro-lensing project (Rucinski 1997a, 1997b) suggest that they are about 3 times more common in space than previously thought. The previous numbers based on the sky-field sample suggested the apparent density of one W UMa system per 1000 normal dwarfs (Duerbeck 1984). The new results imply that the statistics of bright systems is skewed by difficulties of detection of low-amplitude systems, which remain to be discovered in the all sky sample. This sample seems to be complete to relatively bright level of about $V \simeq 8$, where the apparent frequency is indeed about one W UMa system per 300 late-type dwarfs, but shows selection effects for fainter stars.

The above remarks have only a parenthetical significance, as the EUVE sky is limited to the nearest and usually brightest objects. In addition, from the large spectral range observed for the contact binaries, appreciable chromospheric and coronal activity is expected only for the coolest systems. The present paper discusses the EUVE results for two late-type contact binary systems, 44i Bootis B ($P = 0.268$ day) and VW Cephei ($P = 0.278$ day), which had been detected in the EUVE surveys and were judged bright enough for spectral observations. Observations of the third nearby system, ϵ Coronae Austrinae (HR 7152) with the spectral type F and orbital period 0.591

day, were also proposed, but were not granted EUVE time, as the star had not been detected in the surveys. It is not clear whether this non-detection was due to the early spectral type of the star or to its sky position at $(l, b) = (0^\circ, -17^\circ)$, that is toward the “wall” of local absorption in the solar vicinity (Warwick et al. 1993). The EUVE observations of the two contact binaries are compared here with observations of a close, but detached binary ER Vulpeculae ($P = 0.698$ day). This system is frequently wrongly classified as a contact binary, but there is no question that both components are well within their respective Roche lobes (Hill et al. 1990). We note that for all three systems, the orbital periods can be identified with the rotation periods due to synchronization by the tidal forces. In the case of ER Vul, this implies a rotation rate some 40 times faster than solar. For the contact binaries, the rotation is still more rapid reaching some 100-times solar for VW Cep and 44i Boo B. The EUVE observations of the latter star which are described here have already been discussed and interpreted within a context of other active binaries by Dupree (1996a, 1996b).

The paper is organized as follows: Section 2 describes the objects and the observations, and Section 3 discusses the EUV (70 – 140 Å, DSS) light curves. A discussion of the neutral-hydrogen column densities is presented in Section 4. The main discussion of the EUV spectra and the spectroscopic results for the three binary stars is in Section 5. The next Section 6 compares the line-intensity results for the three binary systems and for the rapidly-rotating single star, AB Dor whose EUVE observations were described and analyzed before (Rucinski et al. 1995). The last Section 7 contains conclusions and summary of the paper.

2. EUVE OBSERVATIONS

All the spectral and the Deep Sky Survey data have been processed automatically by the Center for EUV Astrophysics pipeline software to the level Quick Position Oriented Event (QPOE) files. The data have been manually extracted from the QPOE files during a visit to the Center for Extreme-Ultraviolet Astrophysics, Berkeley, California in February 1996. The software version used was #1.6 and the calibration dataset was #1.11. The reasons for re-processing was the usual issue, for EUVE observations, of the optimum placement of the extraction slit, with the added improvement in the Earth blockage temporal filter. The latter was particularly important for the case of VW Cep, as the automatic software rejected a large fraction of data which were obtained at low view angles. The blockage zenith angle was changed uniformly for all data from 98° to 107° .

Several details specific for the program stars as well as for the EUVE observations are listed in Table 1. Since all these stars show period variations, observations of the moments of eclipse centers were collected from the recent literature and initial zero phases and periods were adopted for each star, as in Table 1. This was particularly important for 44i Boo B which, in addition to apparently random period changes, shows a systematic period variation due to the barycentric motion in a visual binary system. For each system, some effort was made to find as recent predictions of the moments of deeper eclipses as possible. The zero phase was then chosen to correspond to moment

just before the start of the EUVE observations so that the calculated phases could be conveniently used as a measure of time within each EUVE run.

The stellar data have been taken from the papers cited below. For estimates of the bolometric fluxes, the formula: $f_{bol} = 2.5 \times 10^{-0.4m_{bol}}$ was used, with $m_{bol} = V_{max} + B.C.$, where the bolometric corrections were from the most recent discussion of Flower (1996). Some additional discussion of distances and maximum magnitudes is in Rucinski (1994).

A few additional details about the three systems and information about timing of their orbital motions are given below:

44i Boo B: The star is the fainter member of the visual binary system ADS 9494. Because of the proximity of the brighter companion of spectral type about G1V, the color and spectral type of the contact binary are uncertain, but must be very late due to shortness of the orbital period. Normally, it is assumed that the contact binary produces all activity-related phenomena, and that the visual companion A does not contribute anything; the same assumption has been made in this paper. The stellar data as well as the distance have been adopted following the extensive discussion by Hill, Fisher & Holmgren (1989a). $B - V \simeq 0.7$ assumed by Rucinski (1994) was probably too blue, and the present entry is still very uncertain. The zero-phase for eclipses was adopted using observations by Rovithis-Livaniou et al. (1995), which was obtained only a few days after the EUVE observations. The period is also from a recent discussion by Opreescu et al. (1996).

VW Cep: There is a faint companion in the system which has been assumed not to contribute to the activity levels observed in the EUVE band. The stellar and distance data are after Hill (1989). The eclipse time prediction was taken from Aluigi et al. (1994) which cites several other recent determinations. This prediction agrees well with continuing observations of VW Cep just before and after the EUVE run by Kiss et al. (1995) and Opreescu et al. (1996).

ER Vul: The system has been extensively studied by Hill, Fisher & Holmgren (1990). The primary-eclipse ephemeride from this paper has been checked against the new determination of Zeinali et al. (1995) and found still applicable.

3. DSS LIGHT CURVES

The complete description of the EUVE instruments is in Bowyer & Malina (1991). The Deep Sky Survey (DSS) channel providing photometric information in the band 70 – 140 Å operated during the spectral observations. It made possible monitoring of the stars for possible flaring activity and for any orbital-phase dependent modulation which could be due to concentration of active regions in some localized areas. The DSS data have been binned into 100 second bins.

Partial bins shorter than 50 seconds have been discarded to ensure reasonable total counts per bin. For all three stars the orbital phases were used as the time coordinates; the relevant data are given in Table 1.

44i Boo B: The light curves are in Figures 1 and 2. The observed count-rate mean and median for 44i Boo were 0.340 and 0.331 counts/sec. Some small activity reaching up to 0.6 counts/sec seemed to be present all the time. Only one moderate brightening at phase about 15.5 was observed. The data plotted in one orbital-phase interval (Fig. 2) show a weak orbital-phase dependence with the lowest count rates at the primary (deeper) eclipse. This eclipse corresponds to occultation of the smaller, slightly hotter component. However, a tendency of the data points to show some grouping in Fig.2 is spurious; it is due to commensurability of stellar and satellite orbits.

VW Cep: The light curves are in Figures 3 and 4. The mean and the median count-rates were 0.088 and 0.083 counts/second. One short flare reaching levels some five times the quiescent level was observed just before the primary eclipse at the phase of about 16.9 (Figure 3). The variability of VW Cep showed no phase relation (Figure 4).

ER Vul: The light curves are in Figures 5 and 6. The mean and the median count rates were 0.146 and 0.143 counts/second. Several short increases in the DSS count rates by about 2 – 3 times the average rate were observed during the run. They seemed to be more frequent in the orbital phases interval around 0.8 to 1.0, i.e. just before the deeper minimum (Figure 6). The quiescent level seemed to show a low-amplitude sinusoidal modulation with a maximum at the orbital phases around 0.2 to 0.3.

The DSS data for all three stars are shown in Figure 7 as histograms of the DSS count rates. The broken lines give the expected Poisson distributions for 100 second intervals based on the mean count rates. Deviations from the Poisson distributions on the side of low counts are due to inclusion of shorter intervals, down to 50 seconds, which led to an increased random noise. The deviations on the high side are due to flaring activity which, as we can see, was moderate in all of the three cases.

Since the DSS data indicated moderate orbital and flaring variability of any of the program stars, the spectral data (Section 5) were analyzed assuming temporal constancy of the signal. However, some tests were made to see if any variability was visible in the strongest spectral lines or in combined spectra binned in four large phase intervals (two eclipses and two maxima). No variability which would be statistically significant was detected, mostly because of the low photon rates.

4. NEUTRAL HYDROGEN ABSORPTION

Estimates of the interstellar hydrogen absorption are needed for interpretation of the spectral data. They have been made using the Center for EUV Astrophysics Internet facility called “ISM Hydrogen Column Density Search Tool” where the database of previous determinations permits their evaluation on the basis of angular and spatial distances from the target object. The database is based on the compilation of Fruscione et al. (1994) with additions from Diplas & Savage (1994). To estimate the monochromatic absorption at a given distance, another Internet facility, called “ISM Transmission Tool” was used, this one being based on the study of Rumph et al. (1994). The assumptions on the relative number of species were: $N(\text{He I})/N(\text{H I}) = 0.1$ and $N(\text{He II})/N(\text{H I}) = 0.01$.

44i Boo B: The column density estimated for most of the neighbor stars is $\log N_H(\text{cm}^2) < 17.4$. This is consistent with the estimates based on X-ray and UV observations by Vilhu & Heise (1986) and Vilhu et al. (1988) of $\log N_H(\text{cm}^2) < 18$. Dupree et al. used $\log N_H(\text{cm}^2) = 18.0$, but this value seems to be too high. We have assumed $\log N_H(\text{cm}^2) = 17.5$ which is consistent with the visibility of emission lines in MW and LW spectra beyond 350 Å.

VW Cep: The database gives very widely scattered determinations of N_H . For a distant star κ Cep (B9III), a few degrees away, $\log N_H(\text{cm}^2) < 18.1$. Vilhu & Heise (1986) give $\log N_H(\text{cm}^2) < 18$. Assuming that the spectrum of VW Cep has similar *relative* intensities of lines as in 44i Boo B for which we assumed $\log N_H(\text{cm}^2) = 17.5$ (Section 5), we obtained $\log N_H(\text{cm}^2) \simeq 18.0$ for VW Cep, the value used hereinafter.

ER Vul: Because of the larger distance than to the two contact binaries, one would expect stronger neutral hydrogen absorption. The database suggests values at the level of $\log N_H(\text{cm}^2) \leq 19$. The X-ray estimate by White et al. (1987) of $N_H(\text{cm}^2) = 6_{-5}^{+14} \times 10^{18}$ permits a very wide range of possibilities, $18 < \log N_H(\text{cm}^2) < 19.3$. The more risky (than for VW Cep) assumption that the overall *relative* line intensities in 44i Boo B and ER Vul are similar (Section 5) leads to an estimate $\log N_H(\text{cm}^2) \simeq 18.5$. For such absorption the emission lines in the MW and LW regions would not be visible, as is actually the case.

5. EUVE SPECTRA

5.1. General properties

The observed spectra are shown in Figures 8 and 9. They are plotted as observed fluxes, uncorrected for neutral-hydrogen absorption. The spectra have been Gaussian smoothed with a filter having $FWHM = 4.7$ pixels for each spectral band (0.0675, 0.135 and 0.270 Å). Thus, they are still slightly over-sampled as the actual resolution was close to 7 original pixels in each of the bands. The spectra show the strong effects of the interstellar absorption for VW Cep and

especially for ER Vul, where even the MW band (170 – 350 Å) is practically devoid of emission lines, in spite of the presence of strong lines in the SW band. The usually very strong He II 304 Å line in ER Vul is absorbed to such a degree that the large Poissonian noise entirely dominates the shape of the line. Only 44i Boo B shows moderate absorption in the MW band and in the short wavelength part of the LW band. The He II 304 Å line is very strong in 44i Boo B and extends beyond the displayed range of the fluxes in Figure 9 with $f_\lambda = 10^{-12}$ erg/cm²/s/Å. The integrated emission line fluxes are listed in Table 2. They are given only for lines for which the formal errors, resulting from combined uncertainties in the line flux as well as in the subtracted background, were smaller than 30%; usually, the errors were at the level of about 10% to 15%.

Because hydrogen absorption is moderate in the SW band (80 – 160 Å) even for relatively large neutral-hydrogen column densities, one can compare directly the spectra in the three studied stars in this spectral region. They turn out quite similar in terms of *relative* strengths of the emission lines. This can be used as a check on our estimates of hydrogen absorption assuming that this similarity extends into the MW and LW regions. The effects of absorption are moderate (factor of less than 3-times) over the wide band between 80 – 450 Å for $\log N_H(\text{cm}^2) < 18$, but become rapidly more severe for higher column densities and longer wavelengths. The estimates of $\log N_H(\text{cm}^2)$ were based on the relative strength of lines in 44i Boo B and the remaining two stars assuming that for the former star, the absorption is $\log N_H(\text{cm}^2) = 17.5$. The results were 18.0 for VW Cep and 18.5 for ER Vul, with uncertainties at the level of 0.3 to 0.5 in $\log N_H$.

5.2. Emission measure solution for 44i Boo B

Our spectra of VW Cep and ER Vul contain too few lines, observed with a too low signal-to-noise ratio to contemplate emission measure determinations. The additional uncertainty is due to the poorly known, but probably large, neutral hydrogen absorption, especially for ER Vul. Only for 44i Boo B the data are of sufficient quality to obtain a differential emission measure distribution. The procedure described by Schmitt et al. (1996) was followed very closely in that only emission lines of various iron ions were used. This way, the large uncertainties related to unknown relative abundances of coronal species become less important. The integral equations for observed flux in line j of the shape: $\phi_j = \frac{1}{4\pi d^2} \int D(T) G_j(T) d \log T$ were approximated by discrete representations: $\phi_j = \frac{1}{4\pi d^2} \sum D(T_i) G_{i,j} \Delta \log T$. The over-determined system of equations was solved using the SVD technique. The solutions were obtained by adding successively more singular values and considering all non-negative DEM distributions with progressively better fit to the data.

We used all 174 lines of iron ions in ionization stages Fe IX to Fe XXIV, as tabulated by Brickhouse, Raymond & Smith (1995). These lines cover formation temperatures within $5.4 < \log T < 7.8$. It should be stressed that we used all the tabulated lines, although the very small subset of only 16 lines had the observed values. The rationale is that the lines which are absent or weak are equally important as those that are observed. In fact, experiments have

shown that solutions based only on visible lines are not sufficiently constrained to the point of becoming basically meaningless. Various values of the temperature increment were tried and a relatively large value $\Delta T = 0.3$ (within $5.7 < \log T < 7.5$) was finally adopted. This gave only 7 discrete values of DEM. We found that solutions with finer sampling or extending too far in the temperature scale would lead to negative values of DEM even for relatively low order of singular values.

The DEM solution is shown in Figure 10. Although the solution looks plausible, we are not satisfied with it for various reasons. The main problem is its uniqueness. The prescription of by Schmitt et al. (1996) invokes buildup of successive approximations of the DEM by inclusion successively more singular values, as long as the resulting function is everywhere positive. In our case, it was found that the first two approximations to the DEM function gave a single peak between $6.0 < \log T < 6.5$. The 3rd solution migrated to higher temperatures with the peak at $\log T \simeq 6.5$, and the 4th and 5th solutions migrated further to give a well defined peak at $\log T \simeq 7.2$. All lower order solutions are confined within the 5th order solution. From the changes in χ^2 , we decided to stop at this point. Also, the still higher-order solutions start giving slightly negative values at $\log T \simeq 5.7 - 6.0$, with no improvement in χ^2 . From the SVD solution and from further experiments with the DEM to spectrum mapping, we got a general impression that the DEM changes quickly at the high-temperature end for relatively small changes in the strength of the “hot” lines of Fe XXIII and Fe XXIV at 132 Å and 192 Å.

We note that the new solution is different from the solution of Dupree et al. (1996) which showed a relatively narrow peak at $\log T \simeq 6.75$, but *both solutions are based on the same observations*. Use of the same hydrogen absorption as that assumed by Dupree et al. of $\log N_H = 18$ (which we feel was too large) does not remove the discrepancy. The solution of Dupree et al. was apparently made by trial and error. We feel that the present solution, which was done in a more objective way, directly shows the difficulty of deriving the DEM from moderate-quality data as those available for 44i Boo B. In particular, the migration of solutions from low-order singular-value solutions concentrated at relatively low temperatures to higher-order solutions encompassing low-order ones, but peaking at higher temperatures directly shows the poor constraining of the problem.

6. COMPARISON OF LOWER CORONA ACTIVITY

The EUVE spectra of 44i Boo B, VW Cep, and ER Vul offer a possibility to compare activity levels of coronal emissions for stars with very short rotation periods below one day. Similar comparisons were frequently made on the basis of IUE and X-ray emissions, culminating in the well-known “saturated-activity” paper of Vilhu & Walter (1987). Here we will augment the new data by the observations of AB Dor, a single rapidly-rotating young star (Rucinski et al. 1995). Its period rotation period of 0.51 day falls approximately half way between the periods of 44i Boo B and VW Cep on one hand and ER Vul on the other hand. All stars have rotation

periods shorter than one day. Of crucial importance is the fact that this is the only single star in the regime of very short periods accessible to EUVE observations. We do not use here the old X-ray observations as they were made with low spectral resolution.

The comparison is made using representative, strong emission features. We use here the Mg II 2800 Å feature for chromospheric plasma at $\log T \simeq 4.2$, the C IV 1550 Å feature for the transition-region plasma at $\log T \simeq 5.1$, both observed with the IUE, adding the new EUVE results for the He II 304 Å line (also formed at about $\log T \simeq 5.1$) and for the strong Fe XXIII 132 Å line which is formed at $\log T \simeq 7.1$. Unfortunately, the gap between $\log T \simeq 5.1$ and $\log T \simeq 7.1$ is very wide: the lines forming at the intermediate temperatures $6.1 < \log T < 6.4$ and visible in EUVE spectra of nearby objects are too heavily absorbed in VW Cep, ER Vul and AB Dor for reasonable comparison. Only the Fe XVI 335 Å line ($\log T \simeq 6.4$) is visible in all four stars, but its strength is very uncertain due to large neutral-hydrogen corrections. The IUE observations were taken from the original sources, frequently cited later in various summary papers: Rucinski & Vilhu (1983), Vilhu & Rucinski (1983), Rucinski (1985c) and Vilhu & Heise (1986).

Figure 11 contains comparison of the four stars in terms of the relative emission-line fluxes, f_{line}/f_{bol} . Arguably, this is the only meaningful quantity which can be used for comparison of contact (44i Boo B, VW Cep) and detached (ER Vul) binary stars with a single (AB Dor) star, as the major differences in the radiating areas are then automatically taken into account. Figure 11 shows that all four stars are practically identical in their chromospheric (Mg II) and transition-region (He II and C IV) emission properties, but relatively large differences are observed in high-temperature emissions. Corrections for the neutral hydrogen absorption are large for the transition-region He II 304 Å line, especially for ER Vul, but we seem to see the same lack of period dependence as observed in the C IV line, which is consistent with the “saturated” regime of activity in these stars. The absorption corrections are even larger for the Fe XVI 335 Å line. In this line, AB Dor seems to be the least active among the four stars. The largest deviation of AB Dor relative to the three binaries is observed for the “hot” line of Fe XXIII at 132 Å. Obviously, without an extensive temporal coverage, it is impossible to tell if AB Dor was observed in a minimum of its dynamo cycle or is always less active than the bracketing (in the period domain) binary stars. We note, however, that Drake (1996) already pointed out that the chromospheric parts of the emission-measure distributions are similar (or predictable) in most active stars, whereas large differences between stars in the emission-measure distributions appear at high temperatures, for $\log T > 10^6$.

7. CONCLUSIONS

Three very close binary stars with the orbital periods shorter than one day, 44i Boo B, VW Cep and ER Vul, show very similar levels of EUV emission line fluxes. The two former are contact binaries with a period close to quarter of a day, the latter is a very close, but detached binary with a the period almost three times longer. During the observations, which consisted of

separate, several days-long, continuous pointings of the EUVE satellite, none of the stars showed large flares or prolonged brightenings; however, the DSS photometry data indicate that low level activity was almost constantly present in each case. These low-level variations were disregarded when forming time-integrated EUV spectra.

The spectra indicate relatively strong neutral hydrogen absorption in the case of VW Cep and especially ER Vul. Thus, it was impossible to attempt differential emission measure determinations for these stars. Such a determination was possible for 44i Boo B, but the quality is moderate (at best) because of the small number of emission lines with well measured fluxes. The solution followed closely the methodology of Schmitt et al.(1996) in that (1) to avoid problems with uncertain relative abundances, only iron lines were used, and (2) the technique of singular-value decomposition was used to prevent over-interpretation of the information content in the spectrum. The result on the differential emission measure (DEM) for 44i Boo B shows lack of any obvious preference of a specific interval of the temperature, with the DEM rising within the accessible interval $6.0 < \log T < 7.2$. The determination strongly depends on inclusion of individual lines so that this determinations of the DEM must be still considered as preliminary.

Strengths of a few strong, well observed emission lines were compared for the three binary stars and for AB Dor, the only single, rapidly-rotating *single* star with the rotation period shorter than one day which is accessible to the EUVE observations (Rucinski et al. 1995). While the emission feature strengths, expressed in f_{line}/f_{bol} , for lines forming at temperatures below $\log T \simeq 5$ show the expected uniformity for all four stars (possibly due to the “saturation”), the hotter lines were observed to be definitely weaker in AB Dor than in the three binaries. It is unclear whether this was due to some temporal variability or is a permanent feature which distinguishes single stars from binaries in this very extreme range of stellar rotation conditions.

Thanks are due to Jeneen Sommers for her help during the reductions of the EUVE data at the Center for EUV Astrophysics.

REFERENCES

- Aluigi, M., Galli, G. & Gaspani, A., 1994, IBVS 4117
- Bowyer, S. & Malina, R. F. 1991, in *Extreme Ultraviolet Astronomy*, eds. R. F. Malina & S. Bowyer, (New York: Pergamon), 397
- Brickhouse, N. S., Raymond, J. C. & Smith, B. W. 1995, *ApJS*, 97, 551
- Diplas, A. & Savage, B. D. 1994, *ApJS*, 93, 211
- Drake, J. J. 1996, in the 9th Cambridge Workshop Cool Stars, Stellar Systems, and the Sun, eds. R. Pallavicini and A. K. Dupree, *ASP Conf Ser*, in press
- Duerbeck, H. W. 1984, *Ap&SS*, 99, 363
- Dupree, A. K. 1996a, in Ninth Cambridge Workshop on Cool Stars, Stellar Systems and the Sun, eds. R. Pallavicini & A. K. Dupree, *ASP Conf. Ser.*, In press
- Dupree, A. K., Brickhouse, N. S. & Hanson, G. J. 1996b, in *Astrophysics in the Extreme Ultraviolet*, eds. S. Bowyer & R. F. Malina, *Kluwer Acad. Publ.*, p.141
- Flower, P. J. 1996, *ApJ*, 469, 355
- Fruscione, A., Hawkins, I., Jelinsky, P & Wiercigroch, A. 1994, *ApJS*, 94, 127
- Hill, G. 1989, *A&A*, 218, 141
- Hill, G., Fisher, W. A. & Holmgren, D. 1989, *A&A*, 211, 81
- Hill, G., Fisher, W. A. & Holmgren, D. 1990, *A&A*, 238, 145
- Kiss, L. L., Gal, J. & Kaszas, G. 1995, IBVS 4181
- Oprescu, G., Dumitrescu, A., Rovithis, P. & Rovithis-Livaniou, H., 1996, IBVS 4307
- Rovithis-Livaniou, H., Rovithis, P., Oprescu, G. & Dumitrescu, A. 1995, IBVS 4172
- Rucinski, S. M. 1985a, in *Interacting Binary Stars*, eds. J.E.Pringle & R.A.Wade, Cambridge Univ. Press, pp.85 & 113
- Rucinski, S. M. 1985b, in *Interacting Binaries*, eds. P.P.Eggleton & J.E.Pringle, Reidel Publ.Co., p.13
- Rucinski, S. M. 1985c, *MNRAS*, 215, 591
- Rucinski, S. M. 1993, in *The Realm of Interacting Binary Stars*, eds. J.Sahade, G.E.McCluskey, Jr. & Kondo, Y., *Kluwer Acad.Publ.*, p.111
- Rucinski, S. M. 1994, *PASP*, 106, 462
- Rucinski, S. M. 1997a, *AJ*, 113, 407
- Rucinski, S. M. 1997b, *AJ*, in press (Mar. 1997; also astro-ph/9611158)
- Rucinski, S. M., Mewe, R., Kaastra, J. S., Vilhu, O. & White, S. M. 1995, *ApJ*, 449, 900 (AB)
- Rucinski, S. M. & Vilhu, O. 1983, *MNRAS*, 202, 1221

- Rumph, T., Bowyer, S. & Vennes, S. 1994, *AJ*, 107, 2108
- Schmitt, J. H. M. M., Drake, J. J., Stern, R. A. & Haisch, B. M. 1996, *ApJ*, 457, 882
- Vilhu, O. & Heise, J. 1986, *ApJ*, 311, 937
- Vilhu, O., Neff, J. E. & Rahunen, T. 1988, in *A Decade of UV Astronomy with IUE*, ESA SP-281, Vol.1, p.299
- Vilhu, O. & Rucinski, S. M. 1983, *A&A*, 127, 5
- Vilhu, O. & Walter, F. M. 1987, *ApJ*, 321, 958
- Warwick 1993, *MNRAS*, 262, 289
- White, N. E., Culhane, J. L., Parmar, A. N. & Sweeney, M. A. 1987, *MNRAS*, 227, 545
- Zeinali, F., Edalati, M. T. & Mirtorabi, M. T. 1995, *IBVS* 4190

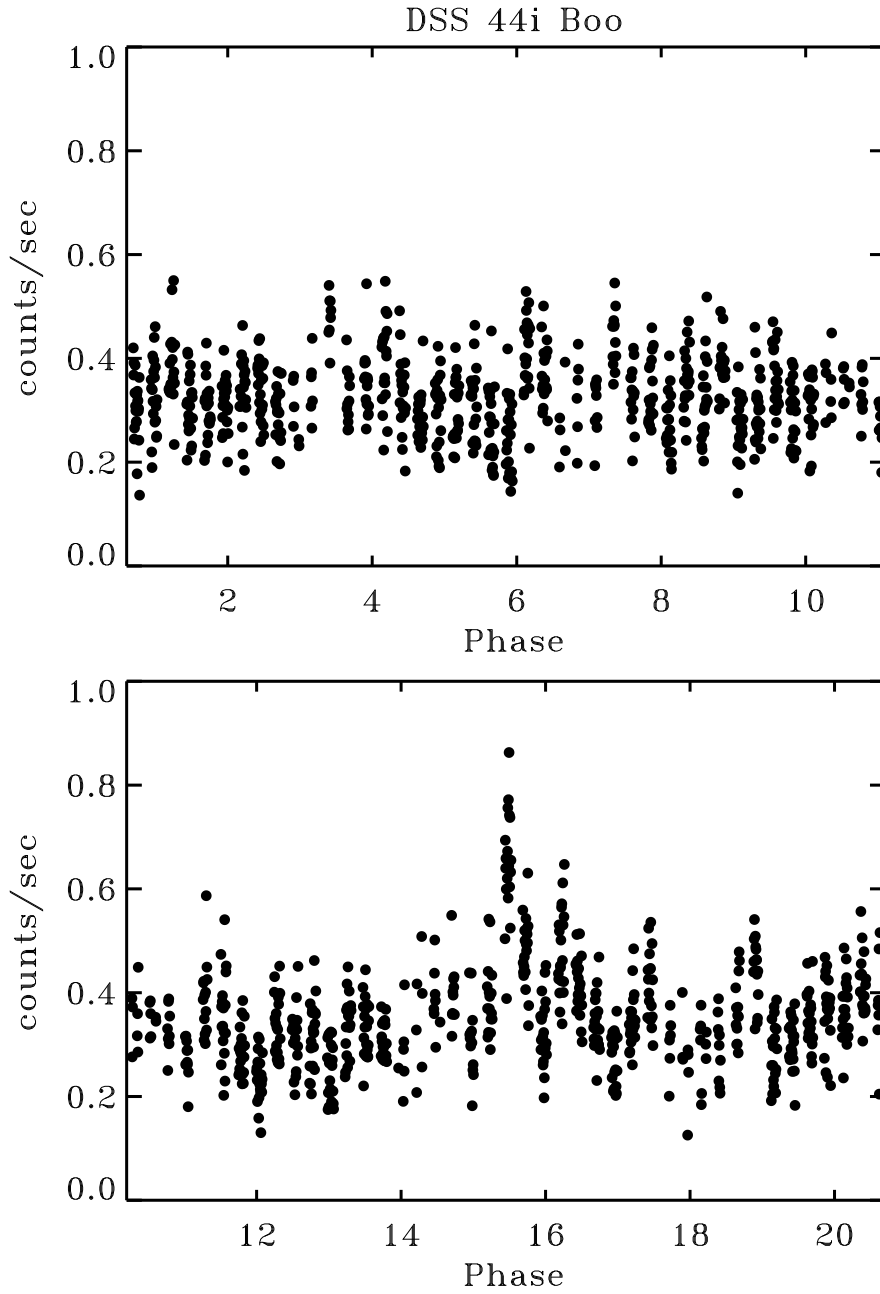


Fig. 1.— The Deep Sky Survey (DSS, 70 – 140 Å) light curve of 44i Boo B. The time scale is in orbital periods counted from the initial epoch, as in Table 1. The data have been binned into 100 second intervals and the bins containing data for more than 50 seconds were used to derive the count rates.

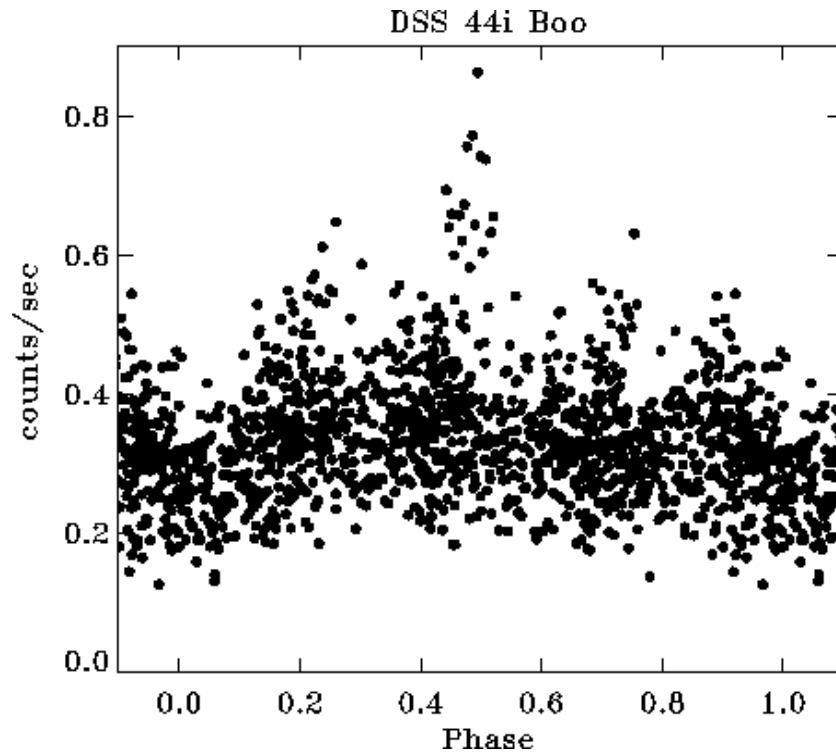


Fig. 2.— The same as in Fig. 1, but with time folded into one orbital period. Note that clumping of the data is due to the commensurability of the binary and satellite periods. However, the tendency for stronger activity at phases around 0.5 seems to be real.

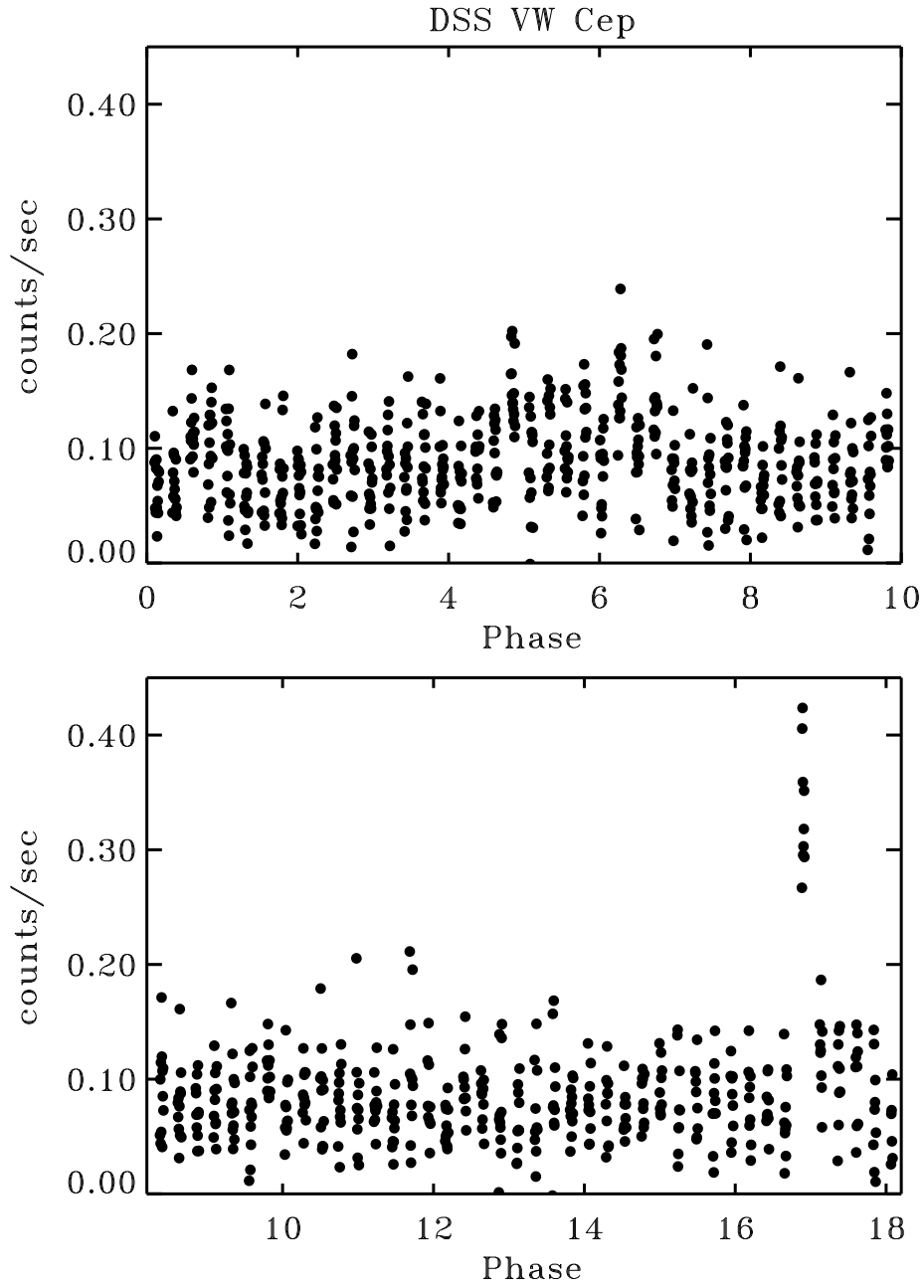


Fig. 3.— The DSS light curve for VW Cep. The system brightened briefly in EUV close to phase the primary eclipse of cycle number 17.

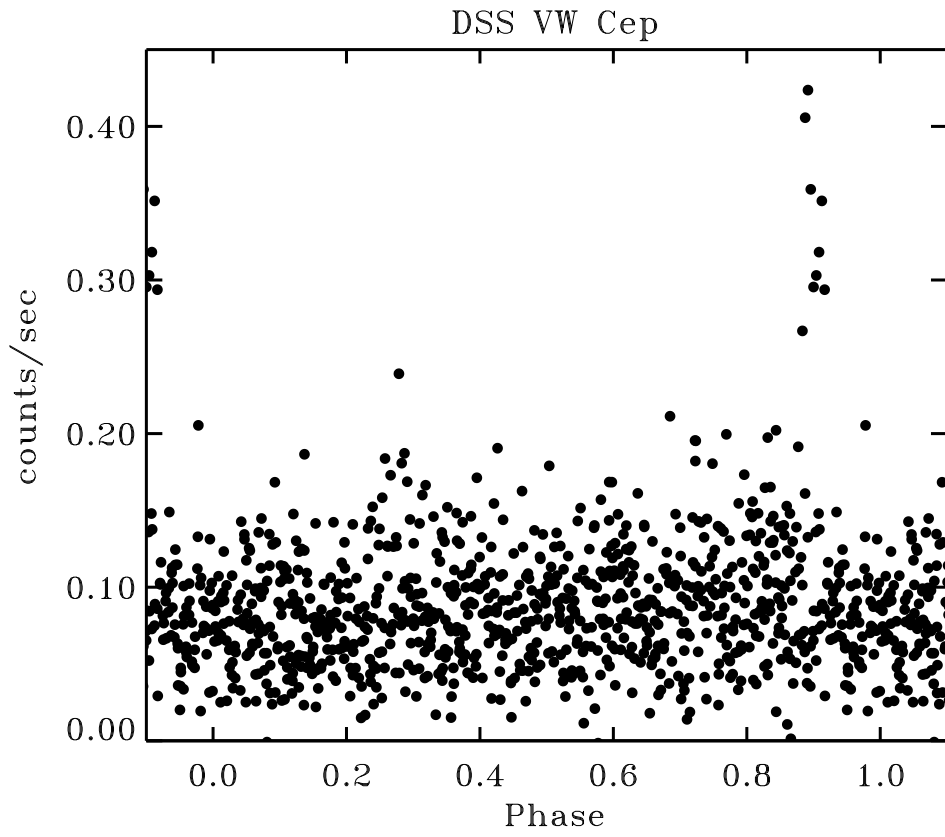


Fig. 4.— The phase-folded light curve for VW Cep.

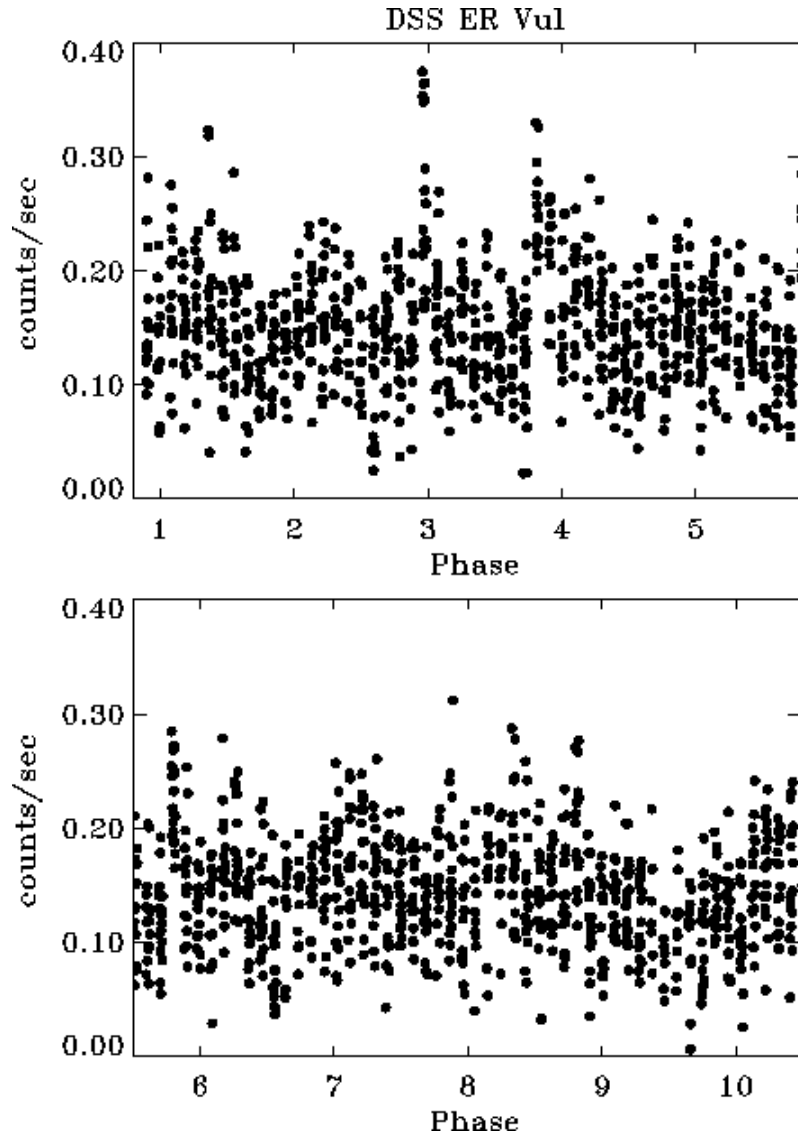


Fig. 5.— The DSS light curve for ER Vul. The system showed some low-level activity most of the time.

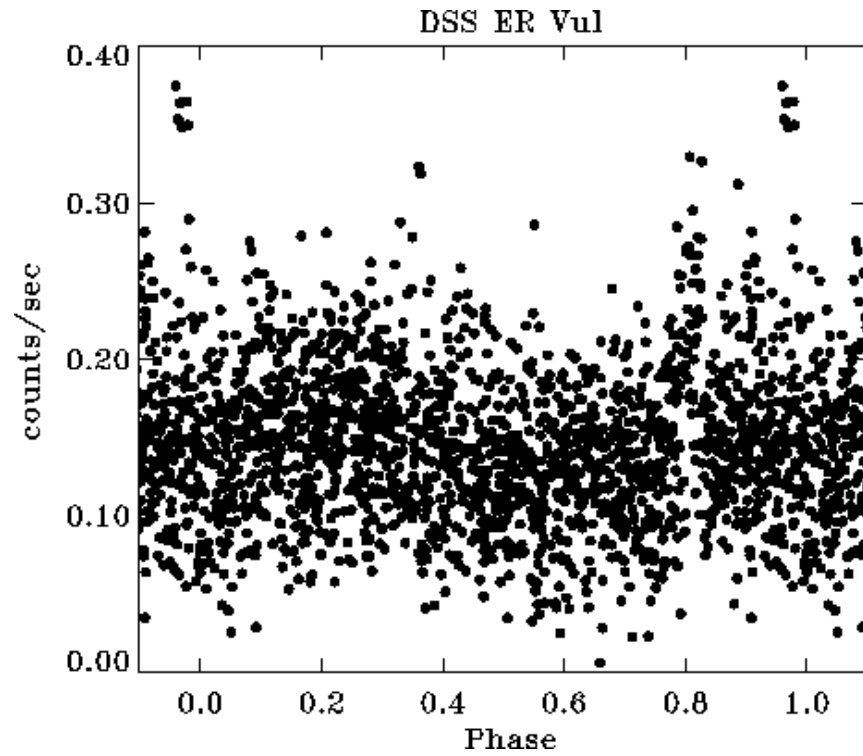


Fig. 6.— The phase-folded light curve for ER Vul. Note that the baseline level was on the average highest at phases close to 0.2 and lowest close to 0.7, while most low-level outbursts took place in the phase interval 0.8 to 1.0.

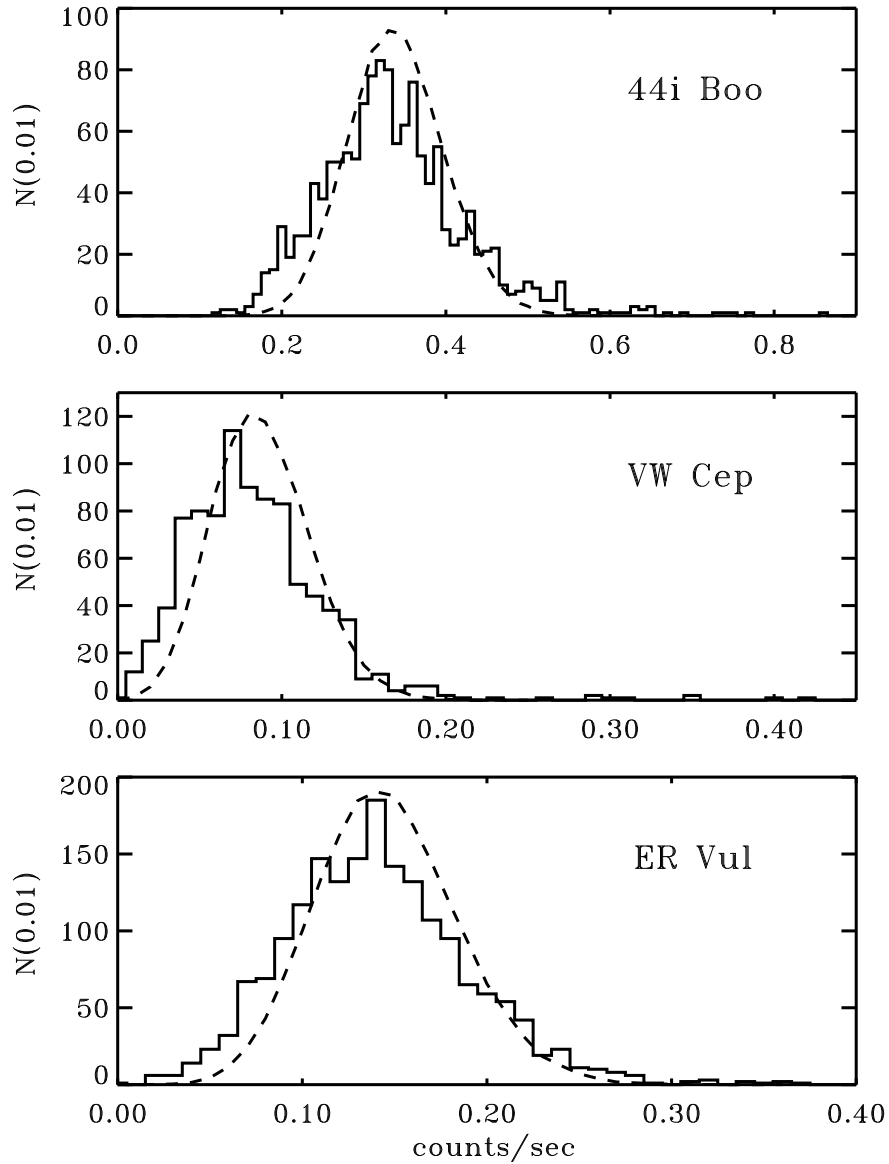


Fig. 7.— Histograms of the DSS count rates for the three program stars. The broken lines give the expected Poissonian distributions evaluated from the mean count rates. The deviations of the observed histograms from the Poisson distributions come from two sources: At the high count rates, they were caused by genuine increases of signal level; at the low count rates the Poisson statistics was corrupted by inclusion of data from shorter time bins (down to 50 sec).

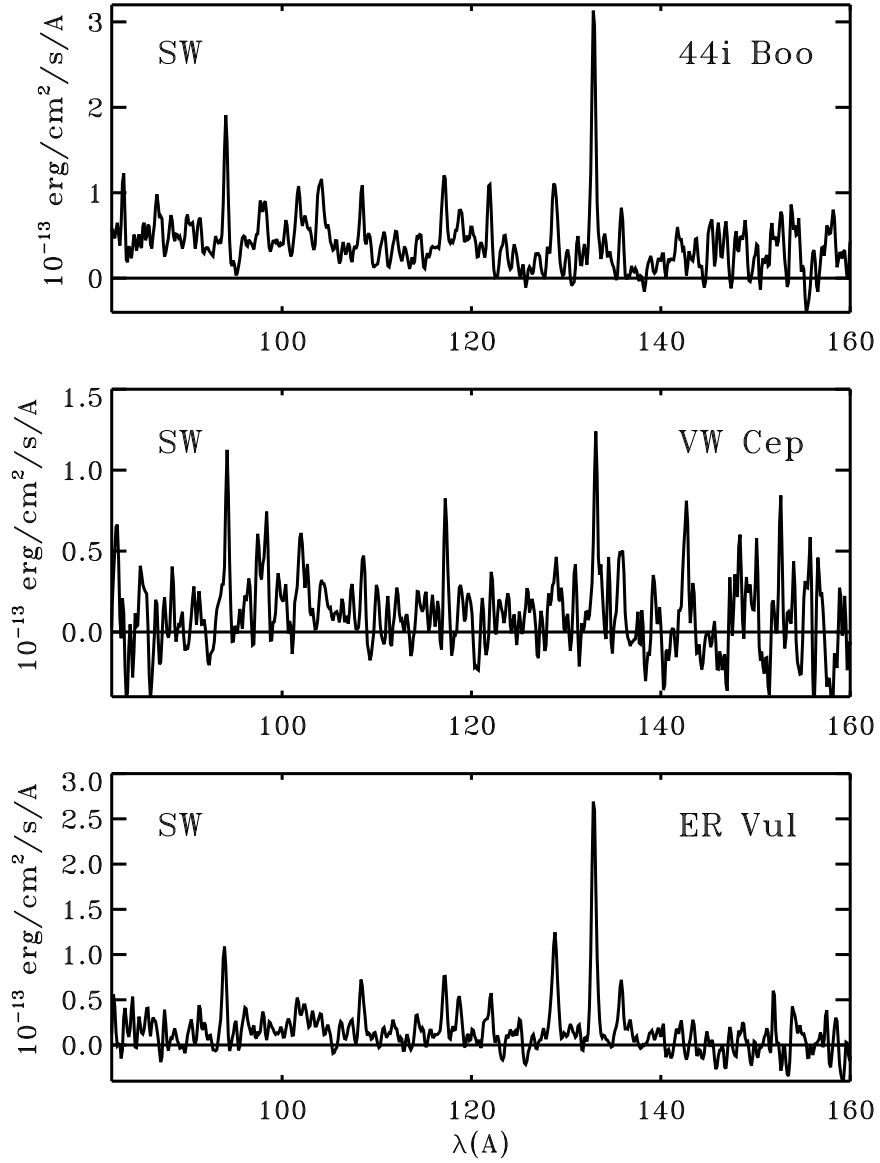


Fig. 8.— The integrated SW spectra of the three program stars expressed in monochromatic fluxes. The units on the vertical axis are $10^{-13} \text{ erg/cm}^2/\text{s}/\text{\AA}$.

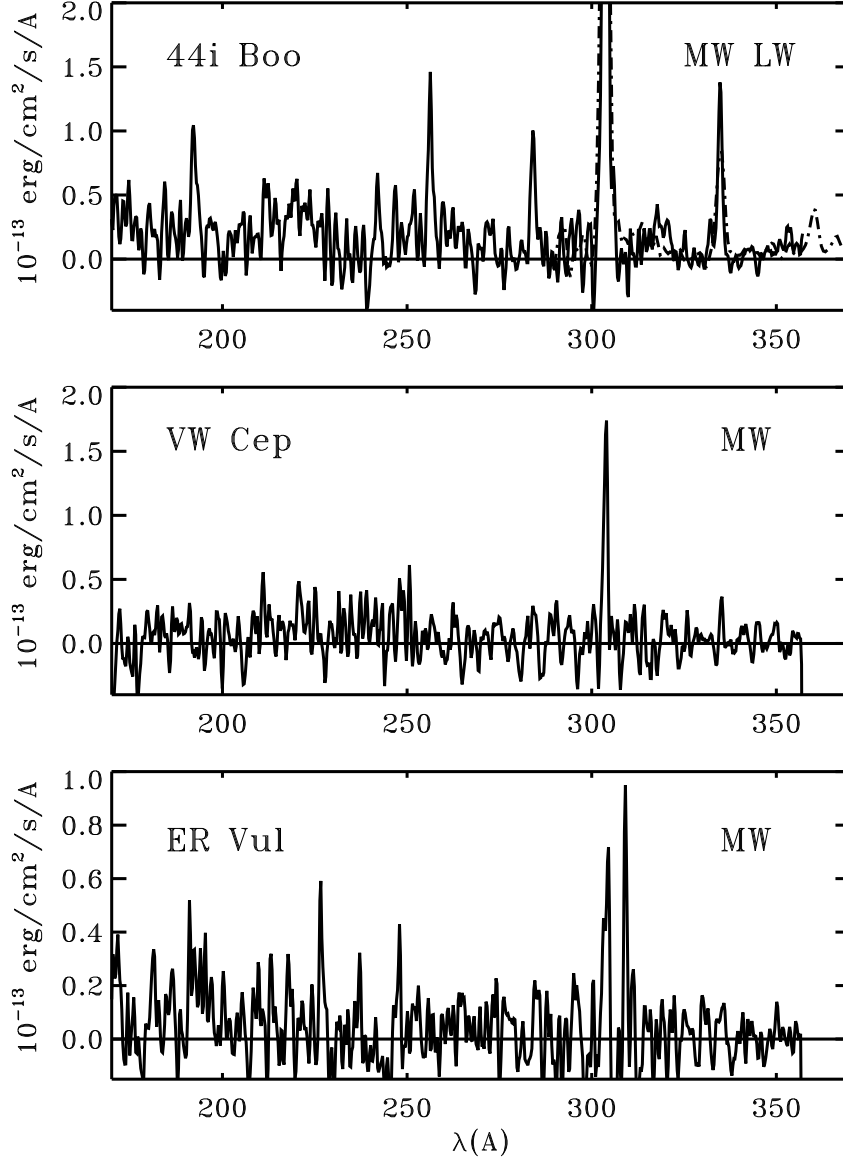


Fig. 9.— The integrated MW spectra of the three program shown in the same format as in Fig. 8. The LW spectrum is over-plotted in the case of 44i Boo (broken line); the other two stars do not show any stellar features in the LW band. Note that for ER Vul, the He II line is corrupted by the large Poissonian fluctuations entering through subtraction of the strong background geocoronal feature.

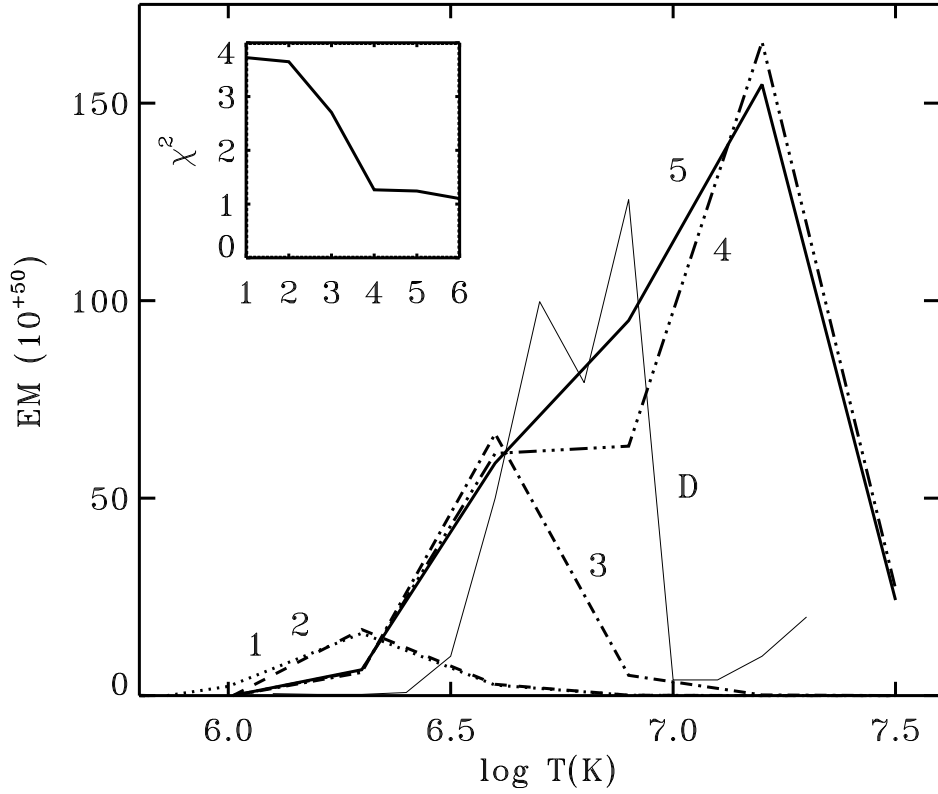


Fig. 10.— The differential emission measure for 44i Boo B evaluated using the approach of successive addition of singular-value solutions, as described in the text. The DEM was derived for 7 independent temperature bins, each $\Delta \log T = 0.3$ wide, without any constraint on the smoothness, but with a requirement of non-negativity, as in Schmitt et al. (1996). Although none of the solutions up to the 5th order would be negative anywhere, they showed no improvement in χ^2 beyond the 4th order. The successive orders are marked by appropriate numbers in the figure and the drop in the χ^2 measure of the fit is shown in the insert. The solution of Dupree et al. (1996) is marked by letter “D” and is shown by the thin line in the figure.

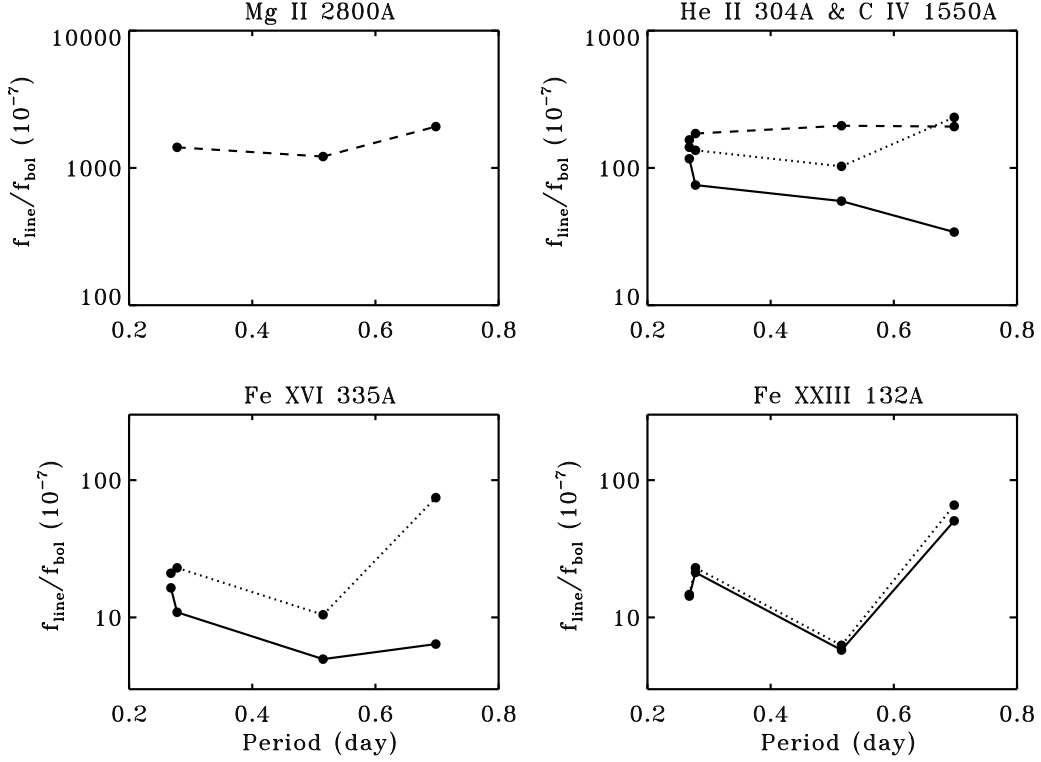


Fig. 11.— Comparison of the relative emission-line fluxes, $f_{\text{line}}/f_{\text{bol}}$, for the three program stars and for AB Dor, a single rapidly-rotating (0.51 day) K-type dwarf. In each panel, the two contact binaries are on the left, ER Vul is on the right, and AB Dor is in the middle. The panels give the relative fluxes for four typical temperatures of line formation: $\log T \simeq 4$ (Mg II 2800 Å), $\log T \simeq 5.0 - 5.1$ (He II 304 Å and C IV 1550 Å), $\log T \simeq 6.4$ (Fe XVI 335 Å) and $\log T \simeq 7.1$ (Fe XXIII 132 Å). The IUE data are connected by broken lines whereas the EUVE data are connected by continuous (observed) and dotted (H I-corrected) lines. The formal measurement errors are not shown as they are usually very small for the strong lines shown here; in fact, systematic errors, which are very difficult to estimate, dominate in determining the uncertainties of the data.

Table 1. Stellar and observation data

| Parameter | 44i Boo B | VW Cep | ER Vul |
|-------------------------------------------------|----------------------|----------------------|----------------------|
| | HD 133640 | HD 197433 | HD 200391 |
| V | (5.9) | 7.30 | 7.25 |
| B-V | (0.8) | 0.85 | 0.59 |
| Sp type | (G8:) | (K0 - K2:) | G1V + G1V |
| Distance (pc) | 13 | 24 | 46 |
| Adopted $\log N_H$ (cm^{-2}) | 17.5 | 18.0 | 18.5 |
| B.C. | -0.2 | -0.24 | -0.06 |
| f_{bol} ($\text{erg}/\text{cm}^2/\text{s}$) | 1.3×10^{-7} | 3.7×10^{-8} | 3.3×10^{-8} |
| Adopted P (day) | 0.26781856 | 0.2783076 | 0.698095 |
| Adopted T_0 (JD) | 2449489.483 | 2448862.521 | 2446328.984 |
| EUVE source | J1503+47.6 | J2037+75.5 | J2102+27.8 |
| EUVE project | 93-013 | 93-013 | 94-011 |
| Start UT (geo) | 2 May 1994 9:38 | 30 Jan 1995 1:29 | 20 Sep 1995 3:25 |
| Stop UT (geo) | 7 May 1994 18:37 | 4 Feb 1995 2:08 | 27 Sep 1995 9:26 |
| Start JD (hel) | 2449474.904 | 2449747.562 | 2449980.646 |
| Stop JD (hel) | 2449480.278 | 2449752.589 | 2449987.897 |
| Nominal exp (sec) | 130,000 | 100,000 | 200,000 |
| Actual exp SW (sec) | 135,462 | 88,951 | 181,394 |
| Actual exp MW (sec) | 132,051 | 88,585 | 179,510 |
| Actual exp LW (sec) | 133,615 | 88,027 | 181,282 |

Note. — See the text for full explanations.

Table 2. Observed EUV emission line fluxes

| Iron ion | band | 44i Boo B | | VW Cep | | ER Vul | | AB Dor | |
|----------|------|-----------------------|--------|-----------------------|--------|-----------------------|--------|-----------------------|--------|
| | | $\lambda(\text{\AA})$ | ϕ | $\lambda(\text{\AA})$ | ϕ | $\lambda(\text{\AA})$ | ϕ | $\lambda(\text{\AA})$ | ϕ |
| 11? | SW | 86.9 | 82 | ... | ... | ... | ... | ... | ... |
| 18 | SW | 94.1 | 109 | 94.2 | 55 | 93.9 | 62 | 94.2 | 22 |
| 21 | SW | 98.0 | 98 | 98.3 | 41 | ... | ... | 98.2 | 13 |
| 19 | SW | ... | ... | ... | ... | 101.6 | 24 | ... | ... |
| 21 | SW | 102.1 | 138 | 102.1 | 61 | 102.3 | 31 | 102.4 | 14 |
| 18 | SW | 104.1 | 103 | 104.3 | 27 | 104.0 | 23 | 104.1 | 10 |
| 19 | SW | 108.4 | 64 | 108.5 | 25 | 108.4 | 43 | 108.5 | 17 |
| 22 | SW | 117.1 | 91 | 117.3 | 35 | 117.1 | 46 | 117.3 | 16 |
| 20 | SW | 118.7 | 76 | ... | ... | 118.7 | 31 | 118.7 | 10 |
| 19 | SW | 120.0 | 57 | ... | ... | ... | ... | ... | ... |
| 20 | SW | 121.9 | 65 | 122.2 | 12 | 121.9 | 35 | 122.0 | 10 |
| 21 | SW | 128.8 | 80 | 128.8 | 35 | 128.8 | 92 | 129.0 | 16 |
| 23 | SW | 132.9 | 186 | 133.2 | 79 | 133.0 | 167 | 133.0 | 35 |
| 22 | SW | 135.9 | 38 | 135.7 | 40 | 135.8 | 45 | 136.0 | 11 |
| 24 | MW | 192.5 | 206 | ... | ... | 191.2 | 40 | 192.2 | 25 |
| 14 | MW | 211.9 | 122 | 211.0 | 52 | ... | ... | 212.1 | 11 |
| He II | MW | 256.4 | 223 | ... | ... | ... | ... | 256.3 | 23 |
| He II | MW | 303.7 | 1580 | 303.7 | 219 | 304.2 | 89 | ... | ... |
| He II | LW | 303.6 | 1454 | 302.8 | 336 | 303.4 | 136 | 303.1 | 344 |
| 16 | MW | 334.8 | 193 | 335.1 | 33 | 335.4 | 17 | 335.1 | 18 |
| 16 | LW | 334.9 | 234 | 333.3 | 48 | 335.4 | 25 | 333.8 | 42 |
| 10 | LW | 353.4 | 42 | ... | ... | ... | ... | 353.8 | 9 |
| 16 | LW | 360.0 | 126 | ... | ... | ... | ... | 359.9 | 16 |
| 12 | LW | 366.2 | 58 | ... | ... | ... | ... | ... | ... |
| 15 | LW | 416.8 | 34 | ... | ... | ... | ... | 416.6 | 18 |

Note. — The emission line fluxes ϕ are in 10^{-15} erg/cm²/s. The empty boxes signify that either the line was not detectable or the measurement carried a formal error larger than 30%.